J. Phys.: Condens. Matter **25** (2013) 216001 (5pp) doi:10.1088/0953-8984/25/21/216001

Conduction electron spin resonance in AlB_2

L M Holanda[1], L Mendonça-Ferreira[2], R A Ribeiro[2], J M Osorio-Guillén[2,3], G M Dalpian[2], K Kuga[4], S Nakatsuji[4], Z Fisk[5], R R Urbano[1], P G Pagliuso[1,5] and C Rettori[1,2]

[1] Instituto de Fisica 'Gleb Wataghin', UNICAMP, 13083-859, Campinas, SP, Brazil
[2] Universidade Federal do ABC, Centro de Ciências Naturais e Humanas, 09210-170, Santo Andre, SP, Brazil
[3] Instituto de Física, Universidad de Antioquia, Medellín, Colombia
[4] Institute for Solid State Physics (ISSP), University of Tokyo, Kashiwa 277-8581, Japan
[5] Department of Physics and Astronomy, University of California Irvine, 92697-4575, Irvine, CA, USA

E-mail: jorge.osorio@fisica.udea.edu.co

Received 22 January 2013, in final form 26 March 2013
Published 30 April 2013
Online at stacks.iop.org/JPhysCM/25/216001

Abstract
This work reports on electron spin resonance experiments in oriented single crystals of the hexagonal AlB_2 diboride compound ($P6/mmm$, $D16h$ structure) which display conduction electron spin resonance. The X-band electron spin resonance spectra showed a metallic Dysonian resonance with g-value and intensity independent of temperature. The thermal broadening of the anisotropic electron spin resonance linewidth ΔH tracks the T-dependence of the electrical resistivity below $T \simeq 100$ K. These results confirm the observation of a conduction electron spin resonance in AlB_2 and are discussed in comparison with other boride compounds. Based on our main findings for AlB_2 and the calculated electronic structure of similar layered honeycomb-like structures, we conclude that any array of covalent B–B layers potentially results in a conduction electron spin resonance signal. This observation may shed new light on the nature of the non-trivial conduction electron spin resonance-like signals of complex f-electron systems such as β-$YbAlB_4$.

(Some figures may appear in colour only in the online journal)

1. Introduction

The family of metallic diborides has attracted great interest from the global scientific community after the discovery of superconductivity in MgB_2 with highest BCS transition temperature, $T_c = 39$ K [1]. It was shown that the transition temperature of MgB_2 decreases by partial substitution of Mg for Al and the superconductivity is totally suppressed for an Al content of 10% [2]. Particularly interesting is the fact that CESR was actually observed in MgB_2 and its behavior was used to directly probe the ce (conduction electrons) and the nature of their interactions [3, 4]. Historically, CESR studies were performed in the early 1950s, 1960s, 1970s and 1980s, for the simple bcc alkali metals, Na [5], Li, K, etc [6], for graphite intercalated compounds (GIC) [7] and other C-based materials [8–10], for the simple fcc metals, Ag, Cu, Al [11] and Pd [12], respectively. However, only in the beginning part of this century were CESR experiments reported in more complex materials such as the binary MgB_2 [3, 4] and the ternary β-$(Yb, Lu)AlB_4$ compounds [13]. A plausible explanation for this fact is related to the complexity of the Fermi surfaces of these metallic compounds which may give rise to a large distribution of g-values as well as the strong spin–orbit scattering of the conduction electrons (ce) responsible for the broadening of the CESR signal (known as the wipe out effect). The combination of these two effects usually set the CESR beyond the detection limit of a conventional ESR spectrometer [8, 14–16], despite the existence of a theoretical prediction of CESR in metals with heavy elements by Fredkin and Freedman based on a model of motional narrowing and many body effects [17, 18].

Nonetheless, in the present work we show that materials such as AlB_2 are good candidates to be CESR active, since they are made out of light constituent elements with a large

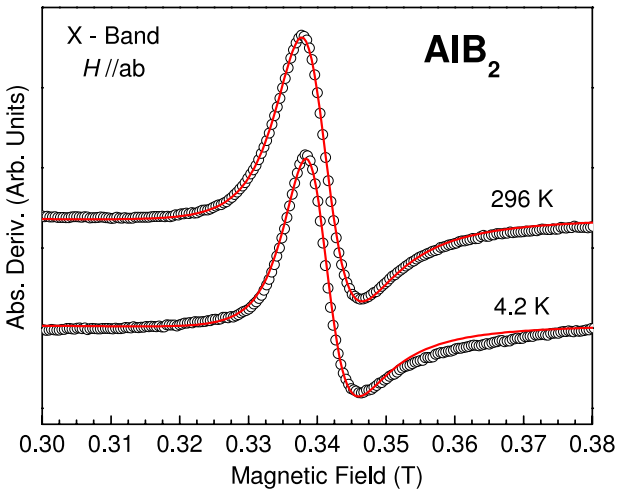

Figure 1. X-band ESR spectra of AlB_2 single crystal with $H \parallel ab$ at 296 K and 4.2 K. The solid (red) lines are fits with a Dysonian lineshape.

Debye temperature and very weak spin–orbit coupling (SOC). The AlB_2 diboride compound (hexagonal structure, space group $P6/mmm$, $D16h$) is formed by rigid boron planes of graphite-type sheets in a honeycomb lattice separated by hexagonal close-packed layers of aluminum [19]. Although the B–B bond distance is similar, the separation between boron planes (along the c-axis) is much larger than the in-plane B–B bonds and changes significantly for different diborides of this family. In particular, the lattice parameters of AlB_2 are $a = 3.08$ Å and $c = 3.24$ Å [20, 21]. Therefore, the electronic properties of AlB_2 turn out to be a quite interesting subject for local probe studies, specially using CESR. Here we claim that our investigation sheds new light on the physical properties of boride systems and provides a further step towards designing new complex materials by combining the architecture of metallic compounds with quite peculiar constituent elements where CESR may be observed. Based on our results, we also suggest that this must be a generic feature in all boride systems.

2. Experimental details

Single crystals of AlB_2 diboride compound were grown using the Al-flux method [22][6]. The crystal structure was determined by x-ray powder diffraction and the single crystals were oriented by Laue method. The X-band ($\nu \approx 9.4$ GHz) CESR experiments were carried out on AlB_2 single crystals in a conventional CW Bruker-ELEXSYS 500 ESR spectrometer using a TE_{102} cavity. The sample temperature was changed by controlling the helium gas-flux and the heat power through an Oxford temperature controller. The angular dependence of the spectra between $H \parallel c$ and $H \parallel ab$ was performed with a goniometer. In-plane electrical resistivity ρ_{ab} was measured in the same crystal in a Physical Property Measurement System—Quantum Design (PPMS-QD) using the standard four-probe method with $H \parallel i_{ab}$.

[6] Single crystals of AlB_2 diboride are commonly grown as by-products of $LuAlB_4$ in Al-flux growth.

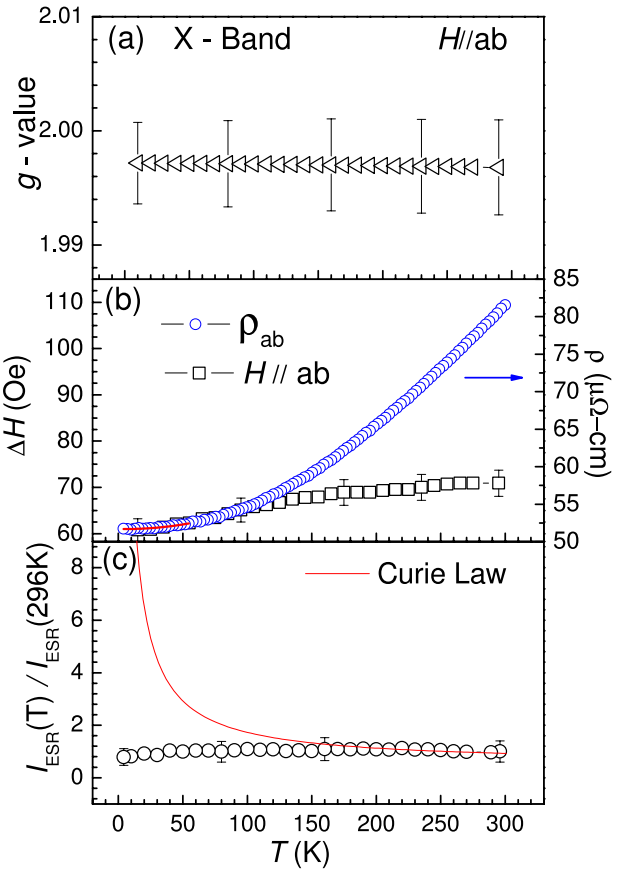

Figure 2. T-dependence of (a) g-value, (b) linewidth, ΔH, and (c) CESR intensity, I, of our AlB_2 single crystal. The in-plane electrical resistivity ρ_{ab} with a T^2 fit are also shown in panel (b). A Curie law is displayed on top of the normalized ESR intensity in the panel (c) in order to emphasize the T-independent behavior of $I_{ESR}(T)/I_{ESR}(296\ K)$.

3. Results and analysis

The ESR spectra of AlB_2 diboride compound at room-T and $T = 4.2$ K are shown in figure 1. A Dysonian lineshape is observed indicating metallic behavior, typical for compounds with skin depth smaller than the size of the sample [6, 23, 24].

From fits of the ESR spectra using a Dysonian line shape [6, 23] we obtained the T-independent g-value of 1.997(4) for $H \parallel ab$ as shown in figure 2(a). This result is very close to the expected one for a free electron $g = 2.0023$ [25]. In figure 2(b) we present the T-dependence of the ESR linewidth, ΔH. The right hand scale of figure 2(b) refers to the in-plane electrical resistivity ρ_{ab} measured at zero magnetic field for our AlB_2 single crystal. The ESR linewidth and ρ_{ab} reasonably follow the same temperature dependence for $T < 100$ K. The solid (red) line is a fit showing that the ρ_{ab} of AlB_2 does display a T^2 behavior at low temperatures as expected in metals. As one can notice, the residual resistivity ratio, $RRR = (\rho_{300\ K} - \rho_{4.2\ K})/\rho_{4.2\ K}$, of 0.5 between room-$T$ and 4.2 K indicating relatively large ce impurity scattering

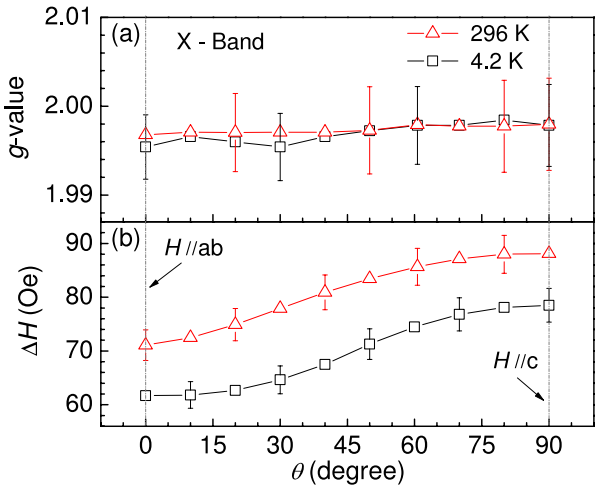

Figure 3. Angular variation of the CESR (a) g-value and (b) linewidth, ΔH, of our AlB_2 single crystal.

in our single crystals. Nonetheless, similar behavior is also observed in polycrystalline AlB_2 samples [20].

Figure 2(c) shows a T-independent ESR intensity calculated from the double integral of the ESR signal. Since the CESR intensity is proportional to the Pauli magnetic susceptibility, $I_{ESR} \propto \chi_P$, if one neglects the small variation of CESR intensity due the fact that the microwave skin depth slightly decreases at low-T as a result of the increase of sample conductivity, the data in figure 2(c) is in good agreement with the susceptibility data of Slusky *et al* for Al content greater than 40% in $Mg_{1-x}Al_xB_2$ [2].

The angular variation of the g-value and linewidth ΔH are presented in figures 3(a) and (b), respectively. The observed g-value is clearly isotropic for the applied magnetic field varying from the ab-plane ($\theta = 0$) towards the c-axis ($\theta = 90°$). Although there is no evident g-value anisotropy within the experimental error bars, the ΔH is anisotropic and roughly 20% broader for $H \parallel c$ when compared to that for $H \parallel ab$. It is not unreasonable to suppose that this fact might be associated with the maximum magnetoresistance along this field orientation which has been already reported for MgB_2 thin films [26]. All these results are clear signatures and typical features of a CESR and thus, our data demonstrate that the resonance observed in AlB_2 is due to the ce in this material.

In figures 4(a)–(c) and 5(a)–(c) we present for AlB_2 and graphite, respectively, the calculated dispersion relation, the site projected density of states (DOS) and the Fermi surface by means of first-principles density functional theory including SOC. We use the full-potential augmented-plane wave method with local orbitals [27] to solve the Kohn–Sham equations and the generalized gradient approximation for the exchange–correlation energy functional [28]. The muffin-tin (MT) radii of Al, B and C are set to $R_{MT}^{Al} = 2.00$ a.u., $R_{MT}^{B} = 1.45$ a.u. and $R_{MT}^{C} = 1.34$ a.u., respectively. The parameter $R_{MT}|\vec{G} + \vec{K}|_{max}$ governing the number of plane waves is chosen to be 8.0. The irreducible wedge of Brillouin zone (IBZ) is sampled with a uniformly spaced $\vec{k}$-grid of $18 \times 18 \times 14$. SOC is included in a second-variational scheme.

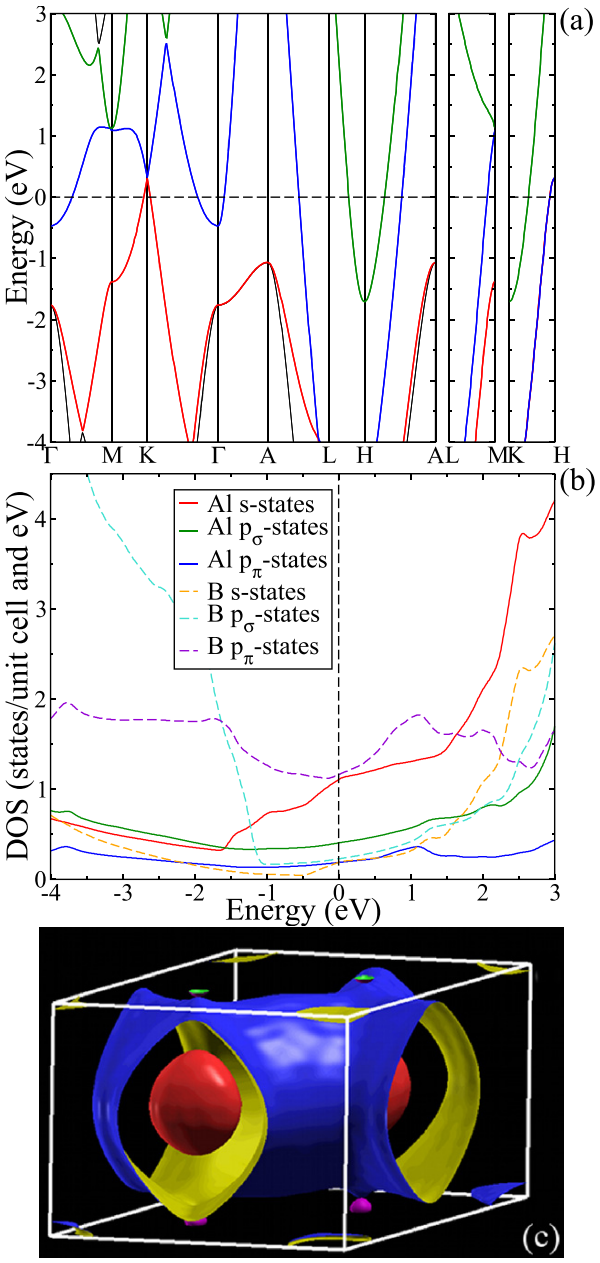

Figure 4. Calculated electronic structure of AlB_2, (a) dispersion relation, (b) site projected DOS and (c) Fermi surface. E_F is represented by a dashed line. The conduction bands crossing E_F in the dispersion relation are highlighted in red, blue and green.

4. Discussion

The regular honeycomb plane structure of boron atoms in AlB_2 and MgB_2 have rather similar ligand bonds, i.e., in-plane σ-bonds and out-of-plane π-bonds. Therefore, it may be expected that these materials would present some similar properties, in particular and noticeably, both of them are active for CESR [3]. The CESR data in these compounds present a relatively narrow ESR line at room-T, $\Delta H \simeq 70$ Oe and 130 Oe for AlB_2 and MgB_2, respectively. The T-dependence of ΔH follows the general trend of the electrical resistivity which is usually associated with ce-phonon scattering via a SOC process [29]. The crystal structure of the AlB_2 and MgB_2

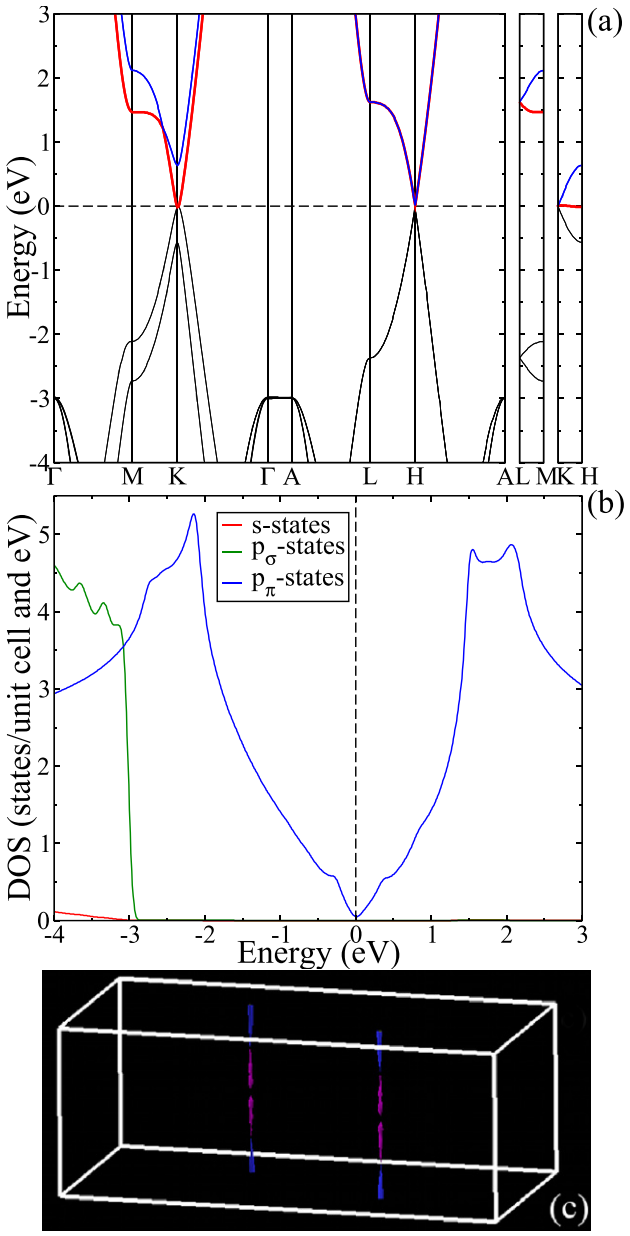

Figure 5. Calculated electronic structure of graphite, (a) dispersion relation, (b) site projected DOS and (c) Fermi surface. E_F is represented by a dashed line.

compounds are reminiscent of that of the GIC, except for the eventual mobility of the intercalated species in GIC [7]. In spite of these similarities, the observed *g*-value anisotropy of graphite [8, 16] is absent in AlB_2, MgB_2 and also in GIC.

From figure 4(a) one can observe that the Fermi level (E_F) is crossed by three conduction bands in all the high symmetry directions of the IBZ. These cbs have a negligible splitting due to the SOC, much less than the splitting produced by the applied magnetic field (∼0.04 meV). From figure 4(b) it is observed that the main contribution to the DOS at E_F is given by the Al s electrons and the B p_π electrons. It is reasonable to assume that the main contribution to the CESR comes from the former fully delocalized ce and the latter ce in the 3D-p_π states that mediate the bonding between the Al e B sheets. We believe that the reason for the observed isotropic CESR *g*-value in this compound is due to the presence of bands with big dispersion across E_F along almost all the high symmetry directions in the IBZ. This fact is in sharp contrast with the case of graphite, where two bands with little dispersion cross E_F along the KH direction (see figure 5(a)). Furthermore, another source for the observed *g*-value isotropy/anisotropy between AlB_2 and graphite is presumable due to the large differences of their Fermi surfaces (see figures 4(c) and 5(c)). We can observe that the Fermi surface of AlB_2 presents four paraboloidal pockets on the bases which come from a conduction band (red band) of B p_π character, the double tube and the features close to the vertices that come from the hybridized Al s, p and B s, p conduction band (blue band), and the quasi-spherical surfaces which come from a conduction band (green band) of Al s character. As a result, the Fermi surface of AlB_2 is much more isotropic in comparison to the one of graphite, which consists of tiny ellipsoidal pockets along the *c*-direction that stem solely from C p_π states.

Moreover, the observation of ESR in the boron layered compounds such as β-$YbAlB_4$ and β-$LuAlB_4$ [13] was recently reported from room-*T* down to 4.2 K. For the case of β-$LuAlB_4$, the resonance behaved as expected for a CESR signal in the entire explored *T*-range, except for the linewidths that were much broader than those observed for the diboride layered compounds. We attribute this broadening to the hybridization of the 3D-p_π bonds in the boron layers with the rare-earth 4f-electrons and to the Fermi surface structure of the heptagon/pentagon architecture of these boride compounds [22]. It is worth mentioning that we have observed distinguished features in the α-$YbAlB_4$ and α-$LuAlB_4$ that are similar to those found in β-$LuAlB_4$ with even broader linewidths [30]. On the other hand, the ESR signal of β-$YbAlB_4$ behaves as CESR at high temperatures (with much narrower ΔH) and acquires signatures of the localized Yb^{3+} magnetic moments at low temperatures as demonstrated by the presence of the hyperfine lines [13]. This dual behavior has attracted great attention and attempts have been made to address some aspects of the CESR-like signal of β-$YbAlB_4$ theoretically very recently [31]. Although the complete understanding of such a CESR-like signal remains unexplained, we strongly believe that our scenario regarding the observation of the CESR in honeycomb-like structured materials will help to shed new light on this issue.

5. Conclusions

In summary we have observed the CESR in AlB_2 with similar features to those reported for the CESR in MgB_2 and GIC. The honeycomb layered structure shared by these materials suggests that the CESR is mainly associated with the fully delocalized Al s electrons hybridized with the electrons in the 3D-p_π bonds of the boron layers. Moreover, the ESR signals that have been observed for β-(Yb, Lu)AlB_4 and α-(Yb, Lu)AlB_4 might be related to the CESR observed for the boron layered structures. Therefore, the results presented in this work lead us to suggest, more generally, that any boron–boron covalent layered material may be a good

candidate to display a CESR signal opening up a new venue for a microscopic investigation by means of a local probe such as ESR. This will be valid though, as long as the architecture of the compound and ce spin-flip scattering via SOC is not too strong because it can dramatically broaden the CESR lines.

Acknowledgments

This work was supported by the auspices of FAPESP (Grant Nos 2006/60440-0, 2007/50986-0, 2011/01564-0, 2012/05903-6), CNPq, FINEP and CAPES (Brazil), and NSF (DMR-0801253) (USA). We would also like to acknowledge financial support from AFOSR MURI-USA.

References

[1] Nagamatsu J, Nakagawa N, Muranaka T, Zenitani Y and Akimitsu J 2001 *Nature* **410** 63
[2] Slusky J S, Rogado N, Regan K A, Hayward M A, Khalifah P, He T, Inumaru K, Loureiro S M, Haas M K, Zandbergen H W and Cava R J 2001 *Nature* **410** 343
[3] Urbano R R, Pagliuso P G, Rettori C, Kopelevich Y, Moreno N O and Sarrao J L 2002 *Phys. Rev. Lett.* **89** 087602
[4] Simon F, Jánossy A, Fehér T, Murányi F, Garaj S, Forró L, Petrovic C, Bud'ko S L, Lapertot G, Kogan V G and Canfield P C 2001 *Phys. Rev. Lett.* **87** 047002
[5] Griswold T W, Kip A F and Kittel C 1951 *Phys. Rev.* **88** 951
[6] Feher G and Kip A F 1955 *Phys. Rev.* **98** 337
[7] Stein R M, Walmsley L, Gualberto G M and Rettori C 1985 *Phys. Rev.* B **32** 4774
[8] Wagoner G 1960 *Phys. Rev.* **118** 647
[9] Jánossy A, Chauvet O, Pekker S, Cooper J R and Forró L 1993 *Phys. Rev. Lett.* **71** 1091
[10] Petit P, Robert J, Yildirim T and Fischer J E 1996 *Phys. Rev.* B **54** 3764
[11] Lubzens D, Shanabarger M R and Schultz S 1972 *Phys. Rev. Lett.* **29** 1387
[12] Monod P 1978 *J. Physique* **39** (Supp. 8) C6-1472
[13] Holanda L M, Vargas J M, Iwamoto W, Rettori C, Nakatsuji S, Kuga K, Fisk Z, Oseroff S B and Pagliuso P G 2011 *Phys. Rev. Lett.* **107** 026402
[14] Elliot R J 1954 *Phys. Rev.* **96** 266
[15] Yafet Y 1963 *Solid State Phys.* **14** 1
[16] Huber D L, Urbano R R, Sercheli M S and Rettori C 2004 *Phys. Rev.* B **70** 125417
[17] Fredkin D R and Freedman R 1972 *Phys. Rev. Lett.* **29** 1390
[18] Freedman R and Fredkin D R 1975 *Phys. Rev.* B **11** 4847
[19] Kortus J, Mazin I I, Belashchenko K D, Antropov V P and Boyer L L 2001 *Phys. Rev. Lett.* **86** 4656
[20] Lal R, Awana V P S, Singh K P, Saxena R B and Kishan H 2006 *Mod. Phys. Lett.* B **20** 989–94
[21] Spear K E 1976 *J. Less-Common Met.* **47** 195–201
[22] Macaluso R T, Nakatsuji S, Kuga K, Thomas E L, Machida Y, Maeno Y, Fisk Z and Chan J Y 2007 *Chem. Mater.* **19** 1918–22
[23] Dyson F J 1955 *Phys. Rev.* **98** 349
Pake G E and Purcell E M 1948 *Phys. Rev.* **74** 1184
[24] Barnes S E 1981 *Adv. Phys.* **30** 801–938
[25] Odom B, Hanneke D, D'Urso B and Gabrielse G 2006 *Phys. Rev. Lett.* **97** 030801
[26] Li Q, Liu B T, Hu Y F, Chen J, Gao H, Shan L, Wen H H, Pogrebnyakov A V, Redwing J M and Xi X X 2006 *Phys. Rev. Lett.* **96** 167003
[27] Dewhurst K, Sharma S, Nordström L and Gross H 2009 http://elk.sourceforge.net
[28] Perdew J P, Ruzsinszky A, Csonka G I, Vydrov O A, Scuseria G E, Constantin L A, Zhou X and Burke K 2008 *Phys. Rev. Lett.* **100** 136406
[29] Schultz S, Dunifer G and Latham C 1966 *Phys. Lett.* **23** 192
[30] Holanda L M *et al* 2013 at press
[31] Ramires A, Coleman P, Nevidomskyy A H and Tsvelik A M 2012 *Phys. Rev. Lett.* **109** 176404